Eur. Phys. J. A **9**, 131–142 (2000)

THE EUROPEAN PHYSICAL JOURNAL A

Semi-inclusive structure functions in the spectator model

A. Bacchetta[1,a], S. Boffi[2], and R. Jakob[3]

[1] Division of Physics and Astronomy, Faculty of Science, Vrije Universiteit De Boelelaan 1081, 1081 HV Amsterdam, The Netherlands
[2] Dipartimento di Fisica Nucleare e Teorica, Università di Pavia and INFN, Sezione di Pavia, Via Bassi 6, 27100 Pavia, Italy
[3] Fachbereich Physik, Universität Wuppertal, Gauss-Straße 20, 42097 Wuppertal, Germany

Received: 26 May 2000
Communicated by Th. Walcher

Abstract. We establish the relationship between distribution and fragmentation functions and the structure functions appearing in the cross-section of polarized 1-particle inclusive deep-inelastic scattering. We present spectator model evaluations of these structure functions focusing on the case of an outgoing spin-$\frac{1}{2}$ baryon. Distribution functions obtained in the spectator model are known to fairly agree at low-energy scales with global parameterizations extracted from totally inclusive DIS data. Therefore, we expect it to give good hints on the functional dependence of the structure functions on the scaling variables x_B, z and on the transverse momentum of the observed outgoing hadron, $\boldsymbol{P}_{h\perp}$. Presently, this dependence is not very well known, but experiments are planned in the near future.

PACS. 13.60.Rj Baryon production – 12.39.-x Phenomenological quark models

1 Introduction

Totally inclusive deep-inelastic scattering (DIS) in the past years provided us with rather precise knowledge of the distribution functions of the proton and the neutron, helping us to understand their inner structure and raising questions yet unanswered. Semi-inclusive DIS displays even richer characteristics. Detecting at least one of the hadrons produced in the high-energy scattering process and measuring its momentum, one is then sensitive not only to the distribution of partons inside the target hadron, but also to the mechanism of hadronization, through which a quark gives rise to a jet of new hadrons. We are then able to measure not only the distribution functions, but also the so-called fragmentation functions. Neither the distribution nor the fragmentation functions can be calculated from first principles within perturbative QCD, because they belong to the non-perturbative realm of bound states. Therefore, models are required.

If only the dominant light-cone component of the momentum of the outgoing hadron is measured, its transverse components being integrated over, then the structure functions appearing in cross-sections will be products of a distribution and a fragmentation function. The already established knowledge of the distribution functions enables one to extract the shape of the fragmentation functions (cf. [1]) and to compare it with other results coming from different experiments, such as electron-positron annihilation.

On the other hand, if we manage to measure the transverse momentum of the outgoing hadron we have the opportunity to study some new interesting distribution and fragmentation functions. In particular, already to leading order in an expansion in powers of $\frac{1}{Q}$ we have access to chiral odd and time-reversal odd functions, as well as functions related to the transverse momentum carried by quarks relative to their parent hadrons momentum [2]. These functions are presently considered to be very interesting and their experimental measurement is in progress (HERMES, COMPASS, RHIC). The only major inconvenience of dealing with cross-sections differential in the transverse momentum of the outgoing hadron is that the structure functions are no more simple products of a distribution and a fragmentation function, but rather convolutions of those.

In this context model evaluations of the structure functions can be very useful. The spectator model proved to be in qualitative agreement with the known (transverse momentum integrated) distribution and fragmentation functions evolved at low energies [3]. Therefore, we expect it to give reasonable estimates for the convolution integrals in semi-inclusive DIS, provided that the inclusion of transverse momentum of partons does not spoil factorization properties, as it is usually assumed [4].

Although our results cannot be considered as highly precise predictions of experimental quantities due to the limitations of the model, we believe them to be relevant, since the spectator model is one of the very few tools available to estimate intrinsic transverse momentum

[a] e-mail: bacchett@nat.vu.nl

distribution without *a priori* assuming a specific form (*e.g.*, Gaussian).

The model incorporates only valence quark distribution and fragmentation, neglecting the presence of sea-quarks, gluons and evolution. Therefore, it is supposed to reproduce the shape of the valence-quark distribution and fragmentation at a low energy scale, which is not known *a priori*. To give an estimate of this scale, one can compare the total momentum carried by quarks as given by the spectator model with the same quantity as given by parameterizations of the distribution functions at a known energy scale. Such a comparison suggests that the spectator model is valid at an energy scale of about 0.2–0.3 GeV.

In principle, the results we obtain need to be evolved to higher energy scales by means of evolution equations for a final comparison with experiment. Evolution equations for transverse momentum dependent functions are not yet known. In this article, therefore, we refrain from taking into account radiative corrections. Nevertheless, we are confident to describe correctly the main features and properties of the structure functions at low (intrinsic) transverse momentum, since perturbative corrections are expected to affect mainly the high transverse momentum tails of these functions.

The spectator model is a semi-phenomenological model, which relies mainly on the idea of describing the hadron as an ensemble of a free parton (struck in the scattering process) and a fictitious, unphysical particle, the spectator, with the right quantum numbers.

The model, at least in its present version, cannot describe time-reversal odd functions, since it does not incorporate final state interactions. On the other hand, the advantages of the model resides in the fact that it is simple, it is covariant and it gives a clear estimate of the distribution of partonic transverse momentum. Last but non least, the model can be treated in wide parts analytically. Some numerical integrations are required only when the cross-section is kept differential also in the transverse momentum of the produced hadron.

In sect. 2 we briefly review the general formalism utilized to treat semi-inclusive DIS, with emphasis on the structure functions calculable using the spectator model. In sect. 3 we present the basic properties of the model and we give the results of our analysis, highlighting what are the broad features that could possibly be observed in experiments.

2 Semi-inclusive DIS

The cross-section for a semi-inclusive DIS event can be written in terms of the contraction between a lepton and a hadron tensor. For instance in the target rest frame we can make use of the formula [5]

$$\frac{\mathrm{d}\sigma}{\mathrm{d}E'\,\mathrm{d}\Omega\,\mathrm{d}^3P_h} = \frac{\alpha^2}{Q^4}\,\frac{E'}{E}\,L_{\mu\nu}W^{\mu\nu}\,, \tag{1}$$

where P_h is the momentum of the outgoing hadron, $Q^2 = -q^2 \geq 0$ is the absolute value of the virtuality of the exchanged photon, $\alpha = e^2/4\pi$ is the fine structure constant, E and E' are the energy of the incident lepton before and after the collision, respectively. $L_{\mu\nu}$ is the lepton tensor and $W^{\mu\nu}$ is the hadronic tensor.

Following a purely phenomenological approach, the hadronic tensor can be parameterized using scalar structure functions. *A priori*, the maximum number of independent structure functions in an arbitrary DIS process is 16. Since we will be interested only in electromagnetic scattering, this number is reduced to 9 by the gauge invariance condition, $q_\mu W^{\mu\nu} = q_\nu W^{\mu\nu} = 0$. A convenient set of functions is formed by the spherical basis structure functions (see, *e.g.*, [6]).

In the spherical basis, constraints coming from angular momentum conservation take a simpler form. From now on, we want to consider only leading terms in an expansion over $\frac{1}{Q}$. In the case of polarized semi-inclusive scattering, helicity conservation considerations allow us to say that five of the structure functions vanish at leading order, leaving only four non-zero structure functions. The complete form of the hadronic tensor at leading order is then

$$W^{\mu\nu} = -g_\perp^{\mu\nu}\frac{W_T}{2} + \mathrm{i}\,\varepsilon_\perp^{\mu\nu}\frac{W'_{TT}}{2} + \left(2\hat{P}_{h\perp}^{\mu}\hat{P}_{h\perp}^{\nu} + g_\perp^{\mu\nu}\right)\frac{W_{TT}}{2} + \hat{P}_{h\perp}^{\{\mu}\varepsilon_\perp^{\nu\}\rho}\hat{P}_{h\perp\,\rho}\frac{\overline{W}_{TT}}{2}, \tag{2}$$

where the curly brackets indicate symmetrization of the indices. For the definitions of the tensor structures appearing in the formula we need to define a normalized time-like and a normalized space-like vector

$$\hat{t}^\mu = \frac{2x_{_B}}{Q}\left(P^\mu - q^\mu\frac{P\cdot q}{q^2}\right), \qquad \hat{q}^\mu = \frac{q^\mu}{Q}\,, \tag{3}$$

by means of which we can define the structures

$$g_\perp^{\mu\nu} = g^{\mu\nu} + \hat{q}^\mu\hat{q}^\nu - \hat{t}^\mu\hat{t}^\nu\,, \tag{4}$$

$$\varepsilon_\perp^{\mu\nu} = \varepsilon^{\mu\nu\alpha\beta}\hat{q}_\alpha\hat{t}_\beta\,, \tag{5}$$

$$\hat{P}_{h\perp}^{\mu} = \frac{g_\perp^{\mu\rho}P_{h\,\rho}}{|g_\perp^{\mu\rho}P_{h\,\rho}|}\,. \tag{6}$$

By calculating the contraction between leptonic and hadronic tensor we can eventually write the following formula for the cross-section [6] in the target rest-frame:

$$\frac{\mathrm{d}\sigma}{\mathrm{d}E'\,\mathrm{d}\Omega\,\mathrm{d}^3P_h} = \sigma_M\,\frac{Q^2}{2|\boldsymbol{q}|^2}\frac{1}{\epsilon} \times\Big\{W_T + \epsilon\big(W_{TT}\cos 2\phi + \overline{W}_{TT}\sin 2\phi\big) + \lambda_e\sqrt{1-\epsilon^2}\,W'_{TT}\Big\}, \tag{7}$$

where λ_e is the helicity of the electron, ϕ is the angle between the scattering plane and the outgoing hadron's momentum (see fig. 1) and where

$$\sigma_M = \frac{4\alpha^2E'^2}{Q^4}\,\cos^2\left(\frac{\theta}{2}\right), \qquad \epsilon^{-1} = 1 + 2\,\frac{|\boldsymbol{q}|^2}{Q^2}\,\tan^2\left(\frac{\theta}{2}\right), \tag{8}$$

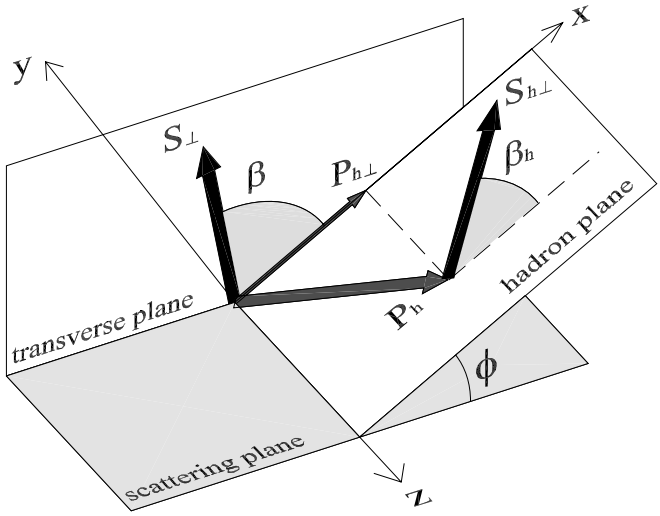

Fig. 1. Sketch of the angles used in the description of the hadronic tensor. The transverse parts of the spin vector of the target, $\mathbf{S}_\perp$, and the momentum and spin vector of the observed hadron, $\mathbf{P_{h\perp}}$ and $\mathbf{S_{h\perp}}$, define the angles β, ϕ and β_h, respectively.

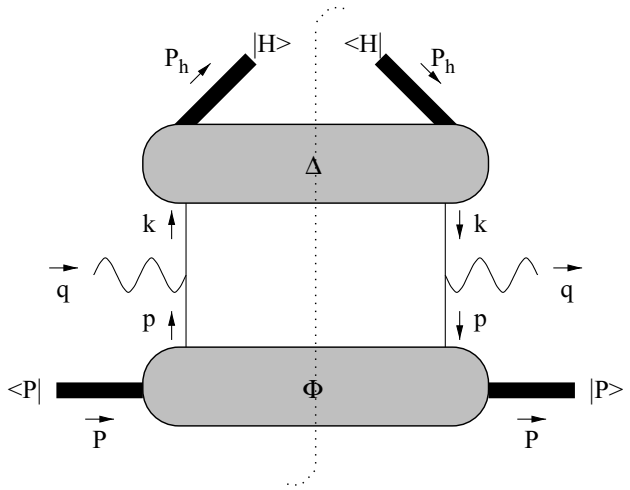

Fig. 2. Diagrammatic representation of semi-inclusive DIS.

θ being the scattering angle of the electron.

When interested in polarization observables of the outgoing particle and/or double polarization measurements one can introduce a compact notation involving the above cross-section and the various observables according to ref. [7]. We do not reproduce it because in the following we only deal with the different structure functions entering the cross-section as well as the expression for the polarization observables. The dominant contribution to the structure functions can be calculated from the cut-diagram shown in fig. 2, representing the hadronic part of a DIS event. According to the usual factorization assumption, the diagram is divided into a hard partonic scattering amplitude and two soft parts, Φ and Δ in fig. 2, called correlation functions. The dominant momentum direction in the upper (lower) part is given by the direction of the outgoing (target) hadron momentum, P_h (P). Quark momenta are almost collinear to their parent hadrons allowing for small transverse components. Using Feynman rules we can give an explicit formula describing the diagram of fig. 2, which represents the hadronic tensor:

$$2MW^{\mu\nu} = \int \mathrm{d}k^+ \, \mathrm{d}^2\boldsymbol{k}_T \, \mathrm{d}p^- \, \mathrm{d}^2\boldsymbol{p}_T \, \delta^{(2)}(\boldsymbol{p}_T + \boldsymbol{q}_T - \boldsymbol{k}_T) \times \sum_q e_q^2 \, \mathrm{Tr}[\Phi_q \, \gamma^\mu \, \Delta_q \, \gamma^\nu] \Big|_{\substack{p^+ = x_B P^+, \\ k^- = P_h^-/z}}, \tag{9}$$

where p and k are the momenta of the quarks respectively before and after absorbing the photon, and the index q denotes quark flavor.

In this formula we use light-cone components of vectors in an infinite momentum frame of reference where the "+" direction is given by the momentum of the target hadron, P, the "−" direction is given by the momentum of the outgoing hadron, P_h, and the photon momentum is purely spatial. In this frame of reference the incident photon has a transverse component, $\boldsymbol{q}_T$. In alternative, one can work with frames of reference where the photon does not have transverse components, which are particularly convenient from the experimental point of view. In such frames the outgoing hadron's momentum acquires a transverse component, which we will denote as $\boldsymbol{P}_{h\perp}$. It can be shown that the relation between these transverse components is [2]:

$$\boldsymbol{q}_T = -\frac{\boldsymbol{P}_{h\perp}}{z}. \tag{10}$$

In eq. (9) the already mentioned correlation functions appear. They are second-rank Dirac tensors defined as [8]

$$\Phi_{q(mn)}(p, P, S) = \int \frac{\mathrm{d}^4\xi}{(2\pi)^4} \mathrm{e}^{-\mathrm{i}p\cdot\xi} \times \langle P, S|\bar\psi^q_{(n)}(\xi) \, \mathcal{L}[\xi, 0; \mathrm{path}] \, \psi^q_{(m)}(0)|P, S\rangle, \tag{11}$$

$$\Delta_{q(mn)}(k, P_h, S_h) = \int \frac{\mathrm{d}^4\xi}{(2\pi)^4} \mathrm{e}^{+\mathrm{i}k\cdot\xi} \times \langle 0|\mathcal{L}[\xi, 0; \mathrm{path}] \, \psi^q_{(m)}(\xi)|P_h, S_h\rangle\langle P_h, S_h|\bar\psi^q_{(n)}(0)|0\rangle, \tag{12}$$

which connect *parton* field operators with *hadron* states, and therefore depend on momenta of the quarks and momenta and spin vectors (S and S_h) of the hadrons. The quark field operators are accompanied by gauge link operators, $\mathcal{L}$, needed to render the correlation functions color gauge-invariant.

If we decompose each correlation function on a basis of 16 Dirac structures, Γ_i, we get the following result:

$$2MW^{\mu\nu} = \sum_{i,j} \frac{\mathrm{Tr}[\Gamma^i \gamma^\mu \Gamma^j \gamma^\nu]}{4} \, 2z \times \int \mathrm{d}^2\boldsymbol{k}_T \, \mathrm{d}^2\boldsymbol{p}_T \, \delta^{(2)}(\boldsymbol{p}_T + \boldsymbol{q}_T - \boldsymbol{k}_T) \sum_q e_q^2 \, \Phi_q^{[\Gamma_i]} \Delta_q^{[\Gamma_j]}, \tag{13}$$

where we defined

$$\Phi_q^{[\Gamma^i]}(x_B, \boldsymbol{p}_T) = \frac{1}{2}\int \mathrm{d}p^-\ \mathrm{Tr}[\Phi_q \Gamma^i]\Big|_{p^+ = x_B P^+} \quad \text{(distribution functions)}, \tag{14}$$

$$\Delta_q^{[\Gamma^i]}(\frac{1}{z}, \boldsymbol{k}_T) = \frac{1}{4z}\int \mathrm{d}k^+\ \mathrm{Tr}[\Delta_q \Gamma^i]\Big|_{k^- = \frac{P_h^-}{z}} \quad \text{(fragmentation functions)}. \tag{15}$$

As a last step, the distribution and fragmentation functions are usually divided in several components, named f_1, g_{1L}, g_{1T}, ... for what concerns the distribution functions, or D_1, G_{1L}, G_{1T}, ... for what concerns the fragmentation functions. We will not pursue the definition of all the possible functions, for which we simply refer to [2]. Note that each function should always carry its flavor index, q, although in the rest of this section we are going to skip it.

Using eq. (13) and comparing it with eq. (2) we can establish relations connecting structure functions to distribution and fragmentation functions. In the following equations we will use the frame of reference and the angles specified in fig. 1. We chose to fix the x-axis in the direction of $\boldsymbol{P}_{h\perp}$ to simplify the formulae. Note that we do not lose generality because in the hadronic tensor there is no dependence on the angle ϕ due to cylindrical symmetry around the z-axis.

To be more concise, we will denote the convolution integral appearing in the hadronic tensor and the summation over quark flavors with the following notation:

$$\mathcal{I}\{\dots\} = \frac{2z}{M}\int \mathrm{d}k_x\,\mathrm{d}k_y\,\mathrm{d}p_x\,\mathrm{d}p_y \times \delta\left(p_x - \frac{|P_{h\perp}|}{z} - k_x\right)\delta(p_y - k_y)\sum_q e_q^2 \dots, \tag{16}$$

where the specific form of the δ-functions is due to relation (10) and to the particular choice of our x-axis.

We are going to divide the structure functions in various contributions arising from particular polarization conditions. Therefore, we are going to label each contribution with two indices, the first one referring to the polarization of the target (U for unpolarized, L for longitudinally polarized, T for transversely polarized) and the second one referring to the polarization of the outgoing hadron. We will not take into account the cases when both hadrons are polarized.

The resulting form of the structure functions is

$$W_T(x_B, z, P_{h\perp}) = W_T^{[\mathrm{UU}]}(x_B, z, P_{h\perp}) + |S_{h\perp}|\sin\beta_h\ W_T^{[\mathrm{UT}]}(x_B, z, P_{h\perp}), \tag{17}$$

$$W_T^{[\mathrm{UU}]}(x_B, z, P_{h\perp}) = \mathcal{I}\{f_1 D_1\}, \tag{18}$$

$$W_T^{[\mathrm{UT}]}(x_B, z, P_{h\perp}) = \mathcal{I}\left\{\frac{k_x}{M_h} f_1 D_{1T}^\perp\right\}, \tag{19}$$

$$W_{TT}(x_B, z, P_{h\perp}) = |S_\perp|\sin\beta\ W_{TT}^{[\mathrm{TU}]}(x_B, z, P_{h\perp}), \tag{20}$$

$$W_{TT}^{[\mathrm{TU}]}(x_B, z, P_{h\perp}) = \mathcal{I}\left\{\frac{k_x}{M_h} h_{1T} H_1^\perp + \frac{k_y p_y p_x + k_x p_y p_y}{2M^2 M_h} h_{1T}^\perp H_1^\perp\right\}, \tag{21}$$

$$W'_{TT}(x_B, z, P_{h\perp}) = \lambda\, W'^{[\mathrm{LU}]}_{TT}(x_B, z, P_{h\perp}) + |S_\perp|\cos\beta\ W'^{[\mathrm{TU}]}_{TT}(x_B, z, P_{h\perp}) + \lambda_h\ W'^{[\mathrm{UL}]}_{TT}(x_B, z, P_{h\perp}) + |S_{h\perp}|\cos\beta_h\ W'^{[\mathrm{UT}]}_{TT}(x_B, z, P_{h\perp}), \tag{22}$$

$$W'^{[\mathrm{LU}]}_{TT}(x_B, z, P_{h\perp}) = \mathcal{I}\{g_{1L} D_1\}, \tag{23}$$

$$W'^{[\mathrm{TU}]}_{TT}(x_B, z, P_{h\perp}) = \mathcal{I}\left\{\frac{p_x}{M} g_{1T} D_1\right\}, \tag{24}$$

$$W'^{[\mathrm{UL}]}_{TT}(x_B, z, P_{h\perp}) = \mathcal{I}\{f_1 G_{1L}\}, \tag{25}$$

$$W'^{[\mathrm{UT}]}_{TT}(x_B, z, P_{h\perp}) = \mathcal{I}\left\{f_1 \frac{k_x}{M_h} G_{1T}\right\}, \tag{26}$$

$$\overline{W}_{TT}(x_B, z, P_{h\perp}) = \lambda\, \overline{W}^{[\mathrm{LU}]}_{TT}(x_B, z, P_{h\perp}) - |S_\perp|\cos\beta\ \overline{W}^{[\mathrm{TU}]}_{TT}(x_B, z, P_{h\perp}), \tag{27}$$

$$\overline{W}^{[\mathrm{LU}]}_{TT}(x_B, z, P_{h\perp}) = \mathcal{I}\left\{\frac{k_x p_x - k_y p_y}{M M_h} h_{1L}^\perp H_1^\perp\right\}, \tag{28}$$

$$\overline{W}^{[\mathrm{TU}]}_{TT}(x_B, z, P_{h\perp}) = \mathcal{I}\left\{\frac{k_x}{M_h} h_{1T} H_1^\perp + \frac{k_x p_x p_x - k_y p_y p_x}{M^2 M_h} h_{1T}^\perp H_1^\perp\right\}. \tag{29}$$

In the previous formulae λ (λ_h) denotes the helicity of the target (outgoing) spin-$\frac{1}{2}$ hadron. The direction of the transverse part of the spin vector $S_\perp$ ($S_{h\perp}$) with reference to the hadron production plane defines the angle β (β_h) as illustrated in fig. 1. The values of the components of the target spin-vector S are known from the preparation of the experiment, whereas those of the S_h have to determined from final state polarimetry. For instance, for self-analyzing hadrons like Λ baryons, the distribution of the products of the weak decay allows the extraction of S_h.

The distribution functions (small letters) are understood to be functions of the variables x_B and $\boldsymbol{p}_T^2$, while the fragmentation functions (capital letters) are understood to be functions of $\frac{1}{z}$ and $\boldsymbol{k}_T^2$.

The functions $D_{1T}^\perp$ and $H_1^\perp$ are time-reversal odd and they cannot be studied in the framework of our model.

For this reason we will only be able to calculate the first term of the structure function W_T and the full structure function W'_{TT}.

Due to eq. (10), integrating over the outgoing hadron transverse momentum, $\boldsymbol{P}_{h\perp}$, corresponds to integrating over $z^2\boldsymbol{q}_T$. Performing this integration leads to a deconvolution of the right-hand side of eq. (13). Consequently, the integrals over $\boldsymbol{p}_T$ and $\boldsymbol{k}_T$ can be performed separately for the distribution and fragmentation functions. Therefore, the structure functions integrated over $\boldsymbol{P}_{h\perp}$ reduce to

$$W_T \ \ (x_B, z) = \frac{1}{M}\, 2z\, f_1(x_B) D_1(\tfrac{1}{z}), \tag{30}$$

$$W'_{TT}(x_B, z) = \frac{\lambda}{M}\, 2z\, g_1(x_B) D_1(\tfrac{1}{z}) + \frac{\lambda_h}{M}\, 2z\, f_1(x_B) G_1(\tfrac{1}{z}), \tag{31}$$

where the new $\boldsymbol{p}_T$ and $\boldsymbol{k}_T$-independent distribution and fragmentation functions are defined as:

$$\begin{aligned} f_1(x_B) &\equiv \int \mathrm{d}^2\boldsymbol{p}_T\ f_1(x_B, \boldsymbol{p}_T^2), \\ g_1(x_B) &\equiv \int \mathrm{d}^2\boldsymbol{p}_T\ g_{1L}(x_B, \boldsymbol{p}_T^2), \\ D_1(\tfrac{1}{z}) &\equiv z^2 \int \mathrm{d}^2\boldsymbol{k}_T\ D_1(\tfrac{1}{z}, \boldsymbol{k}_T^2), \\ G_1(\tfrac{1}{z}) &\equiv z^2 \int \mathrm{d}^2\boldsymbol{k}_T\ G_{1L}(\tfrac{1}{z}, \boldsymbol{k}_T^2). \end{aligned} \tag{32}$$

At this point it is worth to mention that color gauge invariance requires the insertion of link operators in eqs. (14,15) and eqs. (32), whose paths run along a light-like direction from infinity to the point where quark fields are calculated. In the present article we assume that an appropriate choice of gauge is possible to reduce all link operators to unity. For transverse momentum dependent distribution and fragmentation functions this issue is not completely settled in the literature. Some subtle problems can appear at next-to-leading order in $1/Q$. For a discussion of details we refer to [9].

3 Calculation of structure functions

3.1 The spectator model

For a numerical evaluation of the structure functions we will employ the distribution and fragmentation functions as estimated with a spectator model [3]. The basic assumption of the spectator model is that the target hadron can be divided into a quark and an effective spectator state with the required quantum numbers, which is treated to a first approximation as being on-shell with a definite mass. In the case of a baryon target, this second particle is a diquark.

The same idea applies to the hadronization process: the quark fragments into a jet, from which one hadron is eventually detected; the remnants of the jet are treated effectively as an on-shell spectator state. If the detected hadron is a baryon, the second particle is an anti-diquark.

The vertex coupling the baryon to quark and diquark includes a form factor preventing the quark from being far off-shell. The large p^2-behavior of the form factor is controlled by a parameter Λ.

We quote the analytic form of the distribution and fragmentation function we are going to use for numerical evaluation of the structure functions as obtained in [3]. The diquark's spin in the simplest approach can be either 0 (scalar diquark with mass M_s) or 1 (axial vector diquark with mass M_a). For both cases the functions can be cast in the same analytic form where only some parameters take different values. Therefore, we label the functions with an additional index $i \in \{s, a\}$ to distinguish between the two cases. The functions we consider are

$$f_1^i(x_B, \boldsymbol{p}_T^2) = \frac{n_i^2 (1-x_B)^3}{16\pi^3}\, \frac{(m + x_B M)^2 + \boldsymbol{p}_T^2}{(\boldsymbol{p}_T^2 + l_i^2(x))^4}, \tag{33}$$

$$g_{1L}^i(x_B, \boldsymbol{p}_T^2) = a_i\, \frac{n_i^2 (1-x_B)^3}{16\pi^3}\, \frac{(m + x_B M)^2 - \boldsymbol{p}_T^2}{(\boldsymbol{p}_T^2 + l_i^2(x))^4}, \tag{34}$$

$$g_{1T}^i(x_B, \boldsymbol{p}_T^2) = a_i\, \frac{n_i^2 (1-x_B)^3}{16\pi^3}\, \frac{2M(m + x_B M)}{(\boldsymbol{p}_T^2 + l_i^2(x))^4}, \tag{35}$$

$$D_1^i(\tfrac{1}{z}, \boldsymbol{k}_T^2) = \frac{N_i^2 (1-z)^3}{16\pi^3 z^4}\, \frac{(m + \frac{1}{z} M_h)^2 + \boldsymbol{k}_T^2}{(\boldsymbol{k}_T^2 + L_i^2(z))^4}, \tag{36}$$

$$G_{1L}^i(\tfrac{1}{z}, \boldsymbol{k}_T^2) = a_i\, \frac{N_i^2 (1-z)^3}{16\pi^3 z^4}\, \frac{(m + \frac{1}{z} M_h)^2 - \boldsymbol{k}_T^2}{(\boldsymbol{k}_T^2 + L_i^2(z))^4}, \tag{37}$$

$$G_{1T}^i(\tfrac{1}{z}, \boldsymbol{k}_T^2) = a_i\, \frac{N_i^2 (1-z)^3}{16\pi^3 z^4}\, \frac{2M_h(m + \frac{1}{z} M_h)}{(\boldsymbol{k}_T^2 + L_i^2(z))^4}, \tag{38}$$

with the spin factors $a_s = 1$ and $a_a = -\frac{1}{3}$, and where we made use of the newly defined functions:

$$l_i^2(x_B) = \Lambda^2(1 - x_B) + x_B M_i^2 - x_B(1 - x_B) M^2, \tag{39}$$

$$L_i^2(z) = \Lambda^2(1 - \frac{1}{z}) + \frac{1}{z} M_i^2 - \frac{1}{z}(1 - \frac{1}{z}) M_h^2. \tag{40}$$

The values of the parameters of the model have been determined to be

$$\begin{aligned} \Lambda &= 0.5 \text{ GeV}, \\ M_s &= 0.6 \text{ GeV}, \qquad M_a = 0.8 \text{ GeV}, \\ m &= 0.36 \text{ GeV}. \end{aligned} \tag{41}$$

The functions depend only weakly on the chosen value of the quark mass m. The normalization factors n_i and N_i are fixed by the conditions

$$\begin{aligned} \int \mathrm{d}x_B\, \mathrm{d}^2\boldsymbol{p}_T\ f_1^i(x_B, \boldsymbol{p}_T^2) &= 1, \\ \int \mathrm{d}z\, \mathrm{d}^2\boldsymbol{k}_T\ z\, \left(z^2 D_1^i(\tfrac{1}{z}, \boldsymbol{k}_T^2)\right) &= 1. \end{aligned} \tag{42}$$

Note that for the fragmentation function the normalization condition is put on the first moment.

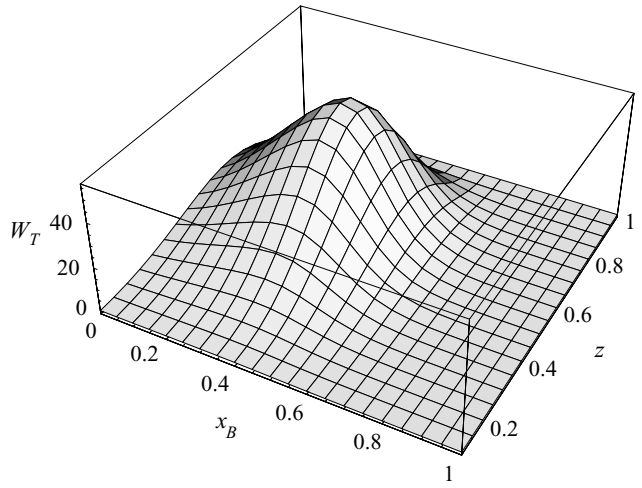

Fig. 3. Dependence of the structure function $W_T^{[\mathrm{UU}]}$ on x_B and z at $P_{h\perp} = 0$.

At this point, it is appropriate to make some comments on the results of the model as compared to a Gaussian distribution of intrinsic transverse momentum. First of all, the spectator model is covariant, while the Gaussian approach is not. Secondly, once the parameters are chosen to properly describe longitudinal momentum distributions, the model intrinsically describes transverse momentum distributions without any further "ad hoc" assumption. These distributions can be significantly different from the Gaussian ones, as we will show in sect. 3.2, not only in the behaviour at high transverse momentum, which is anyway affected by perturbative corrections. Moreover, the model suggests different transverse momentum dependences for different distribution and fragmentation functions, whereas a Gaussian approach does not.

We gave the distribution and fragmentation functions for scalar and axial-vector diquarks. We must now address the problem of defining the hadron state in terms of the quark-diquark content. From a group theory analysis, for a proton, a neutron and a Λ-particle the results are [10]:

$$\begin{aligned}
|p\rangle &= \tfrac{1}{\sqrt{2}}|u,S\rangle + \tfrac{1}{\sqrt{6}}|u,A\rangle - \tfrac{1}{\sqrt{3}}|d,A\rangle,\\
|n\rangle &= \tfrac{1}{\sqrt{2}}|d,S\rangle - \tfrac{1}{\sqrt{6}}|d,A\rangle + \tfrac{1}{\sqrt{3}}|u,A\rangle,\\
|\Lambda\rangle &= \tfrac{1}{\sqrt{12}}|u,S\rangle - \tfrac{1}{\sqrt{12}}|d,S\rangle\\
&\quad -\tfrac{2}{\sqrt{12}}|s,S\rangle + \tfrac{1}{\sqrt{4}}|u,A\rangle - \tfrac{1}{\sqrt{4}}|d,A\rangle.
\end{aligned} \tag{43}$$

Using these results, the probability of finding an up, down or strange quark in one of these hadrons is related to the probability of finding a scalar or axial-vector diquark in the following way:

$$\begin{aligned}
f_1^{p\to u} &= \tfrac{3}{2}f_1^s + \tfrac{1}{2}f_1^a, & f_1^{p\to d} &= f_1^a,\\
f_1^{n\to u} &= f_1^a, & f_1^{n\to d} &= \tfrac{3}{2}f_1^s + \tfrac{1}{2}f_1^a,\\
f_1^{\Lambda\to u} &= \tfrac{1}{4}f_1^s + \tfrac{3}{4}f_1^a, & f_1^{\Lambda\to d} &= \tfrac{1}{4}f_1^s + \tfrac{3}{4}f_1^a,\\
f_1^{\Lambda\to s} &= f_1^a.
\end{aligned} \tag{44}$$

Overall normalizations ensure the correct number sum rules for valence quarks in the baryons. Analogous formulae hold for all other distribution functions and for the fragmentation functions as well.

Once we have computed the distribution and fragmentation functions for a scalar and axial-vector diquark, we can eventually calculate the argument of the convolutions occurring in the structure functions for a given process. At this stage, the (charge squared weighted) sum over quark flavors is rewritten in a weighted sum over the different diquark species:

$$\sum_q e_q^2 f_1^q D_1^q = \sum_{i,j=s,a} c_{ij}\, f_1^i D_1^j, \tag{45}$$

where the coefficients depend on the type of hadrons involved.

For instance, for the following processes:

– $e\,p \to e'\,\Lambda\,X$

$$\begin{aligned}
&\frac{4}{9}f_1^{p\to u}D_1^{u\to\Lambda} + \frac{1}{9}f_1^{p\to d}D_1^{d\to\Lambda} =\\
&\frac{1}{6}f_1^s D_1^s + \frac{1}{2}f_1^s D_1^a + \frac{1}{12}f_1^a D_1^s + \frac{1}{4}f_1^a D_1^a;
\end{aligned} \tag{46}$$

– $e\,p \to e'\,p'\,X$

$$\begin{aligned}
&\frac{4}{9}f_1^{p\to u}D_1^{u\to p} + \frac{1}{9}f_1^{p\to d}D_1^{d\to p} =\\
&f_1^s D_1^s + \frac{1}{3}f_1^s D_1^a + \frac{1}{3}f_1^a D_1^s + \frac{2}{9}f_1^a D_1^a;
\end{aligned} \tag{47}$$

– $e\,n \to e'\,\Lambda\,X$

$$\begin{aligned}
&\frac{4}{9}f_1^{n\to u}D_1^{u\to\Lambda} + \frac{1}{9}f_1^{n\to d}D_1^{d\to\Lambda} =\\
&\frac{1}{24}f_1^s D_1^s + \frac{1}{8}f_1^s D_1^a + \frac{1}{8}f_1^a D_1^s + \frac{3}{8}f_1^a D_1^a;
\end{aligned} \tag{48}$$

– $e\,n \to e'\,p\,X$

$$\begin{aligned}
&\frac{4}{9}f_1^{n\to u}D_1^{u\to p} + \frac{1}{9}f_1^{n\to d}D_1^{d\to p} =\\
&\frac{1}{6}f_1^s D_1^a + \frac{2}{3}f_1^a D_1^s + \frac{5}{18}f_1^a D_1^a.
\end{aligned} \tag{49}$$

Analogous formulae apply to other combinations of distribution and fragmentation functions.

In the following section we will concentrate only on the first process. However, using appropriate coefficients c_{ij} and appropriate hadron masses one can carry out the calculations for any baryon-to-baryon process.

3.2 Numerical results for structure functions in $e\,p \to e'\,\Lambda\,X$

In this section we present numerical results for structure functions of the process $e\,p \to e'\,\Lambda\,X$ obtained using the distribution and fragmentation functions from the spectator model. We concentrate on Λ production, since it is

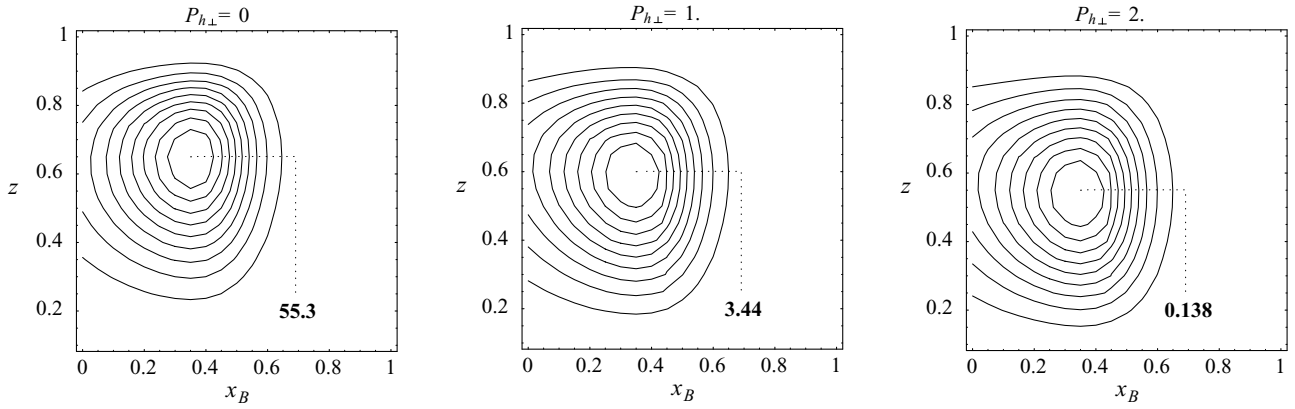

Fig. 4. Contour-plot of the structure function $W_T^{[\mathrm{UU}]}$ for different values of $P_{h\perp}$ (GeV). Numbers inside the plot area denote the height of maxima. Spacing between isometric lines corresponds to 10 % of maximum height.

possible to determine its polarization from the kinematics of its decay. We will consider separately different experimental situations with or without polarization of the target and of the produced Λ. In this way the various terms in eq. (17) and eq. (22) can be accessed.

1 – Unpolarized proton target and unpolarized produced Λ. We performed the calculation of the structure function $W_T^{[\mathrm{UU}]}$ of eq. (18) using f_1 from eq. (33) and D_1 from eq. (36), with the coefficients c_{ij} as specified in eq. (46). After integrating over k_x and k_y by using the δ-function, we obtain

$$
\begin{aligned}
&W_T^{[\mathrm{UU}]}(x_{_B}, z, P_{h\perp}) = \\
&\sum_{i,j=s,a} c_{ij}\, \tfrac{n_i^2 N_j^2}{2M\,(2\pi)^6}\, (1-x_{_B})^3 \left(\frac{1-z}{z}\right)^3 \\
&\times \int \mathrm{d}p_x\, \mathrm{d}p_y\, \frac{(m+x_{_B}M)^2 + p_x^2 + p_y^2}{\left[p_x^2 + p_y^2 + l_i^2(x)\right]^4} \\
&\times \frac{\left(m + \frac{1}{z}M_h\right)^2 + \left(p_x - \frac{|P_{h\perp}|}{z}\right)^2 + p_y^2}{\left[\left(p_x - \frac{|P_{h\perp}|}{z}\right)^2 + p_y^2 + L_j^2(z)\right]^4}.
\end{aligned}
\tag{50}
$$

The remaining integration has been carried out numerically making use of an adaptive multi-dimensional integration method. As we remarked before, integrating out $P_{h\perp}$ leads to a deconvolution and, consequently, the transverse momentum integration can be performed separately for the distribution and fragmentation functions as shown in eq. (30). With the form of the functions given by the spectator model the integrations can be carried out analytically [3]. Comparison of those analytical results with the outcome of a numerical integration has been used as a check of consistency. The results are displayed in the plots. Figure 3 shows the structure function $W_T^{[\mathrm{UU}]}$ at $P_{h\perp} = 0$. Figure 4 shows the contour-plot of the same function at three different values of $P_{h\perp}$. An interesting feature is that when $P_{h\perp}$ increases, the position of the peak slowly moves to lower values of z, while there is no change in the x position of the peak. In other words, a hadron produced with a higher transverse momentum is more likely to carry a lower fraction of the longitudinal momentum of the original quark. We remark that this behavior is due to the kinematical conditions imposed by momentun conservation. In fig. 5 we show the result obtained by integrating the structure function over z.

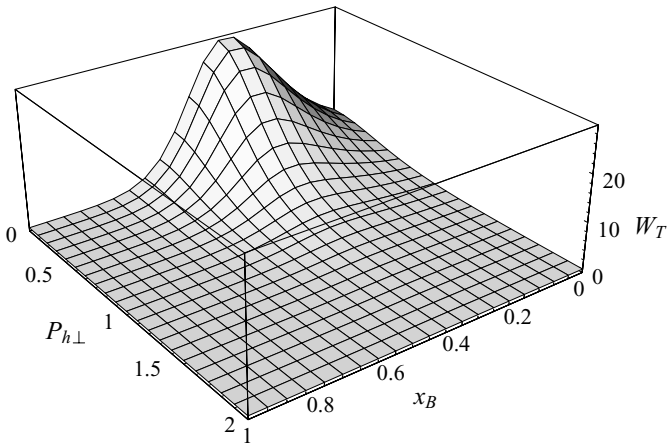

Fig. 5. Dependence of the structure function $W_T^{[\mathrm{UU}]}$ on the outgoing hadron transverse momentum, $P_{h\perp}$ (measured in GeV) and the fractional momentum $x_{_B}$.

In fig. 6 we show the result of integrating the structure function over $x_{_B}$ and we compare it with the same structure function obtained by assuming a Gaussian distribution of transverse momentum, *i.e.* (cfr. [2])

$$
\begin{aligned}
&W_T^{[\mathrm{UU}]}(z, P_{h\perp}) = \\
&2\pi \sum_{i,j=s,a} c_{ij}\, D_1^j(z)\, \frac{1}{z^2}\, \mathcal{G}\left(\frac{P_{h\perp}}{z}\,; \langle|p_T|\rangle^2 + \langle|k_T|\rangle^2\right),
\end{aligned}
\tag{51}
$$

where

$$
\begin{aligned}
&\mathcal{G}\left(\frac{P_{h\perp}}{z}\,; \langle|p_T|\rangle^2 + \langle|k_T|\rangle^2\right) = \\
&\frac{1}{\pi\,(\langle|p_T|\rangle^2 + \langle|k_T|\rangle^2)}\, \exp\left(-\frac{P_{h\perp}^2}{z^2(\langle|p_T|\rangle^2 + \langle|k_T|\rangle^2)}\right).
\end{aligned}
$$

We chose the values of $\langle|p_T|\rangle$ and $\langle|k_T|\rangle$ to be equal to 0.5

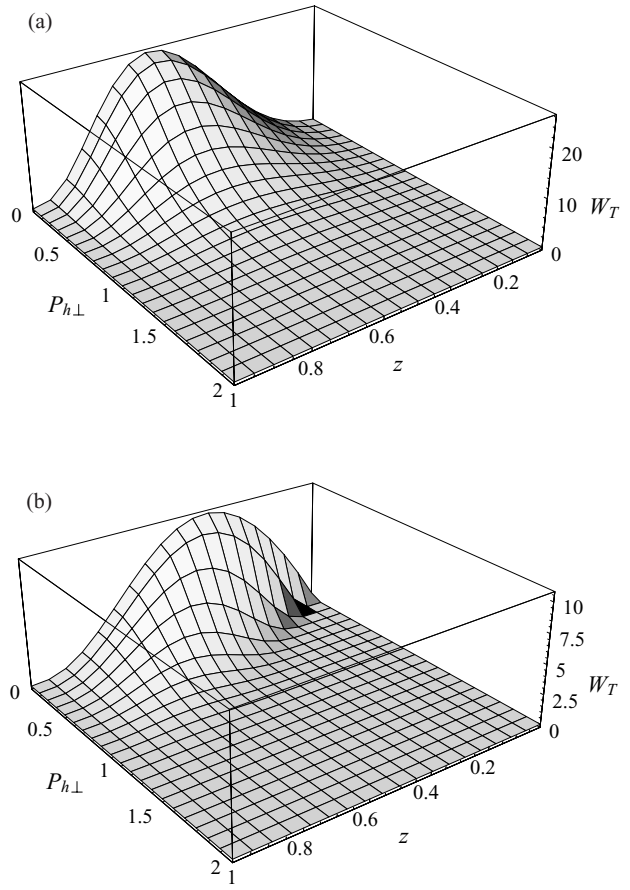

Fig. 6. Dependence of the structure function $W_T^{[\mathrm{UU}]}$ on the outgoing hadron transverse momentum, $P_{h\perp}$ (measured in GeV) and the fractional momentum z: (a) spectator model, (b) Gaussian distribution with $\langle|p_T|\rangle = \langle|k_T|\rangle = 0.5$ GeV.

GeV. Higher values produce a broader distribution. The behaviour of the structure function shows clear differences between the diquark model and the Gaussian predicitions, especially in the low-z region. We have checked that this holds true for different assumed values for $\langle|p_T|\rangle$ and $\langle|k_T|\rangle$ in a realistic range. Finally, we can integrate over both z and x_B at the same time, thereby obtaining the dependence of the structure function $W_T^{[\mathrm{UU}]}$ on $P_{h\perp}$ alone. In fig. 7 we present the result of this integration as compared to the results coming from a Gaussian ansatz with $\langle|p_T|\rangle = \langle|k_T|\rangle = 0.3$ GeV and $\langle|p_T|\rangle = \langle|k_T|\rangle = 1$ GeV . The diquark model shows a quite distinct behaviour with respect to the first Gaussian, while it is not very different from the second one.

2 – Longitudinally polarized proton target and unpolarized produced Λ. In this case, we need to calculate the structure function $W'^{[\mathrm{LU}]}_{TT}$ of eq. (23). Using eq. (34) and eq. (36) and integrating over k_x and k_y using the δ-

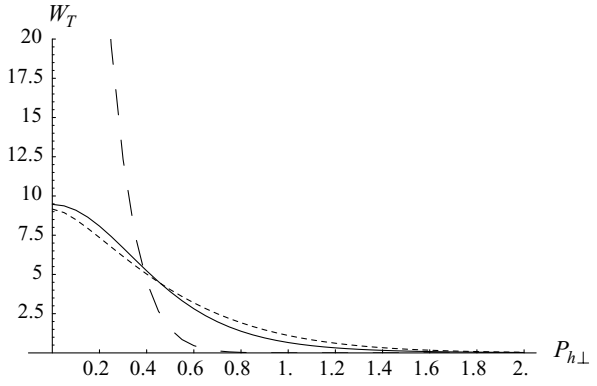

Fig. 7. Dependence of the structure function $W_T^{[\mathrm{UU}]}$ on the outgoing hadron transverse momentum, $P_{h\perp}$ (GeV), from the spectator model (solid line) and Gaussian ansatz with $\langle|p_T|\rangle = \langle|k_T|\rangle = 0.3$ GeV (long-dashed line) and $\langle|p_T|\rangle = \langle|k_T|\rangle = 1$ GeV (short-dashed line).

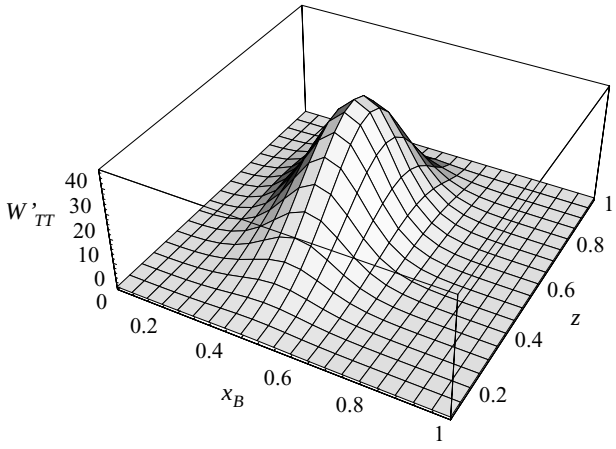

Fig. 8. Dependence of the structure function $W'^{[\mathrm{LU}]}_{TT}$ on x_B and z at $P_{h\perp} = 0$.

functions, we obtain the formula

$$W'^{[\mathrm{LU}]}_{TT}(x_B, z, P_{h\perp}) = \sum_{i,j=s,a} c_{ij}\, a_i\, \frac{n_i^2 N_j^2}{2M\,(2\pi)^6}\,(1-x_B)^3 \left(\frac{1-z}{z}\right)^3 \times \int \mathrm{d}p_x\, \mathrm{d}p_y \frac{(m+x_B M)^2 - p_x^2 - p_y^2}{\left[p_x^2 + p_y^2 + l_i^2(x)\right]^4} \times \frac{\left(m + \frac{1}{z}M_h\right)^2 + \left(p_x - \frac{|P_{h\perp}|}{z}\right)^2 + p_y^2}{\left[\left(p_x - \frac{|P_{h\perp}|}{z}\right)^2 + p_y^2 + L_j^2(z)\right]^4}. \quad (52)$$

Figure 8 shows the structure function $W'^{[\mathrm{LU}]}_{TT}$ at $P_{h\perp} = 0$. Figure 9 shows the contour-plot of the same function at three different values of $P_{h\perp}$. As in the case of $W_T^{[\mathrm{UU}]}$, for increasing $P_{h\perp}$ the position of the peak moves to lower values of z. Integration over z or x_B produces a behavior similar to the one shown in fig. 5. Integrating over both z and x_B we obtain the dependence of the structure function $W'^{[\mathrm{LU}]}_{TT}$ on $P_{h\perp}$ alone (fig. 10).

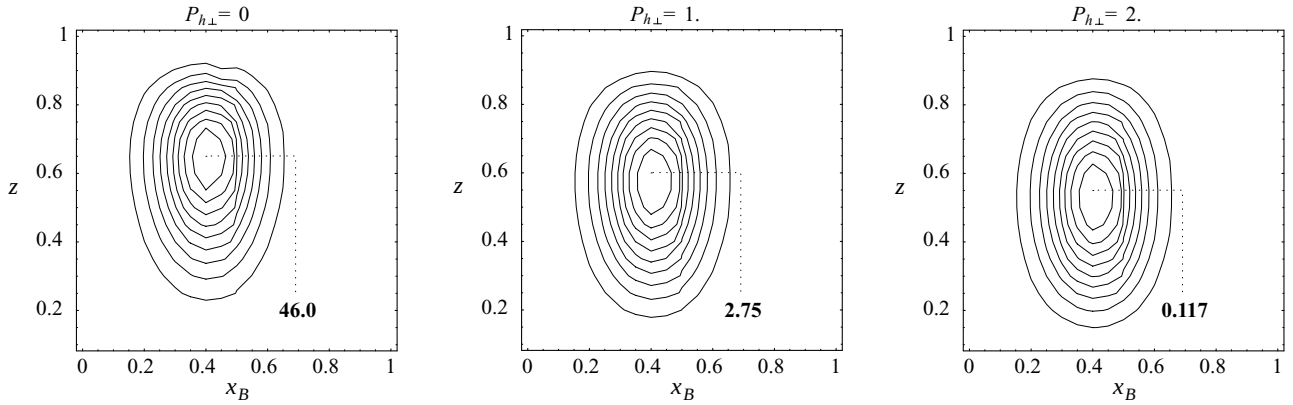

Fig. 9. Contour-plot of the structure function $W'^{[\mathrm{LU}]}_{TT}$ for different values of $P_{h\perp}$ (GeV). Numbers inside the plot area denote the height of maxima. Spacing between isometric lines corresponds to 10 % of maximum height.

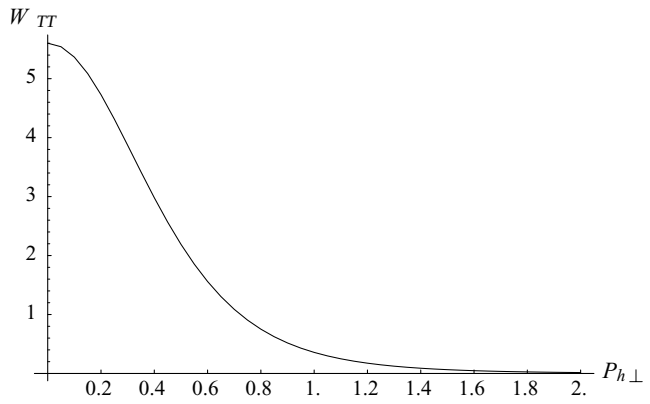

Fig. 10. Dependence of the structure function $W'^{[\mathrm{LU}]}_{TT}$ on the outgoing hadron transverse momentum, $P_{h\perp}$ (GeV).

3 – Transversely polarized proton target and unpolarized produced Λ. Substituting the results coming from eq. (35) and eq. (36) in eq. (24) and integrating over k_x and k_y we obtain

$$W'^{[\mathrm{TU}]}_{TT}(x_B, z, P_{h\perp}) = \sum_{i,j=s,a} c_{ij}\, a_i\, \frac{n_i^2 N_j^2}{2M\,(2\pi)^6}\,(1-x_B)^3 \left(\frac{1-z}{z}\right)^3 \times \int \mathrm{d}p_x\,\mathrm{d}p_y \frac{2\,p_x\,(m+x_B M)}{\left[p_x^2+p_y^2+l_i^2(x)\right]^4} \times \frac{\left(m+\frac{1}{z}M_h\right)^2 + \left(p_x - \frac{|P_{h\perp}|}{z}\right)^2 + p_y^2}{\left[\left(p_x - \frac{|P_{h\perp}|}{z}\right)^2 + p_y^2 + L_j^2(z)\right]^4}. \quad (53)$$

Figure 11 shows the structure function $W'^{[\mathrm{TU}]}_{TT}$ at $P_{h\perp} = 0.4$ GeV. Fig. 12 shows the contour-plot of the same function at three different values of $P_{h\perp}$. Again, as $P_{h\perp}$ increases the position of the peak moves to lower values of z.

Integrating over both z and x_B we obtain the dependence of the structure function $W'^{[\mathrm{TU}]}_{TT}$ on $P_{h\perp}$ alone (fig. 13).

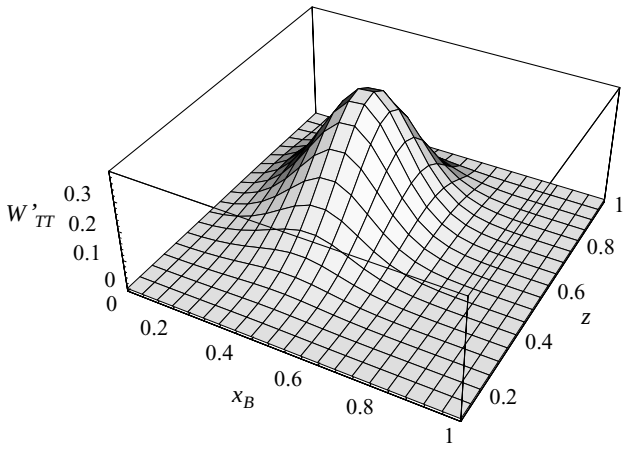

Fig. 11. Dependence of the structure function $W'^{[\mathrm{TU}]}_{TT}$ on x_B and z at $P_{h\perp} = 0.4$ GeV.

4 – Unpolarized proton target and longitudinally polarized produced Λ. Substituting the results coming from eq. (33) and eq. (34) in eq. (25) and integrating over k_x and k_y, we obtain

$$W'^{[\mathrm{UL}]}_{TT}(x_B, z, P_{h\perp}) = \sum_{i,j=s,a} c_{ij}\, a_j\, \frac{n_i^2 N_j^2}{2M\,(2\pi)^6}\,(1-x_B)^3 \left(\frac{1-z}{z}\right)^3 \times \int \mathrm{d}p_x\,\mathrm{d}p_y \frac{(m+x_B M)^2 + p_x^2 + p_y^2}{\left[p_x^2+p_y^2+l_i^2(x)\right]^4} \times \frac{\left(m+\frac{1}{z}M_h\right)^2 - \left(p_x - \frac{|P_{h\perp}|}{z}\right)^2 - p_y^2}{\left[\left(p_x - \frac{|P_{h\perp}|}{z}\right)^2 + p_y^2 + L_j^2(z)\right]^4}. \quad (54)$$

Figure 14 shows the structure function $W'^{[\mathrm{UL}]}_{TT}$ at $P_{h\perp} = 0$ and at $P_{h\perp} = 0.5$ GeV. In this case, the contributions containing the negative a_a factor play a larger role than in the previous cases. For this reason, the significance of the contour plots is reduced and we preferred to show 3-D plots of the structure function.

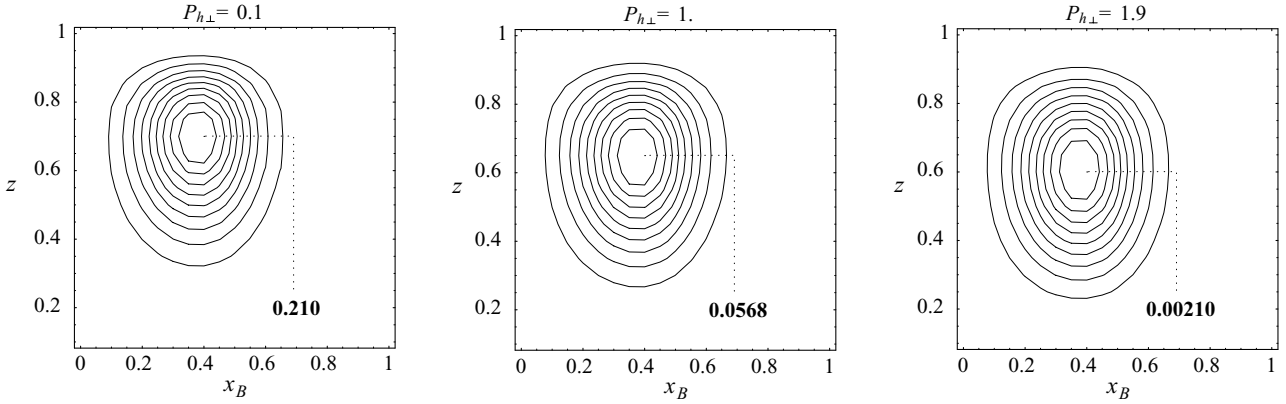

Fig. 12. Contour-plot of the structure function $W'^{[\mathrm{TU}]}_{TT}$ for different values of $P_{h\perp}$ (GeV). Numbers inside the plot area denote the height of maxima. Spacing between isometric lines corresponds to 10 % of maximum height.

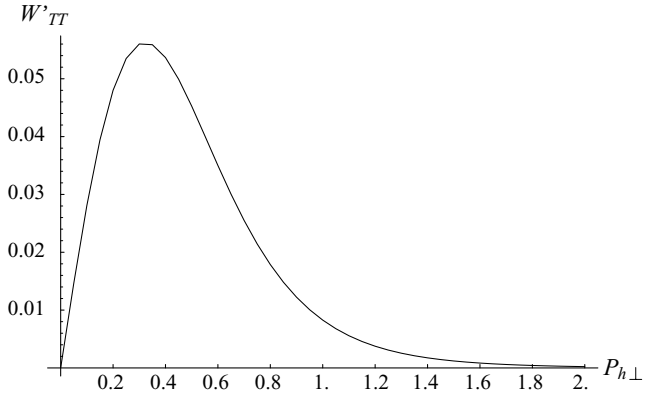

Fig. 13. Dependence of the structure function $W'^{[\mathrm{TU}]}_{TT}$ on the outgoing hadron transverse momentum, $P_{h\perp}$ (GeV).

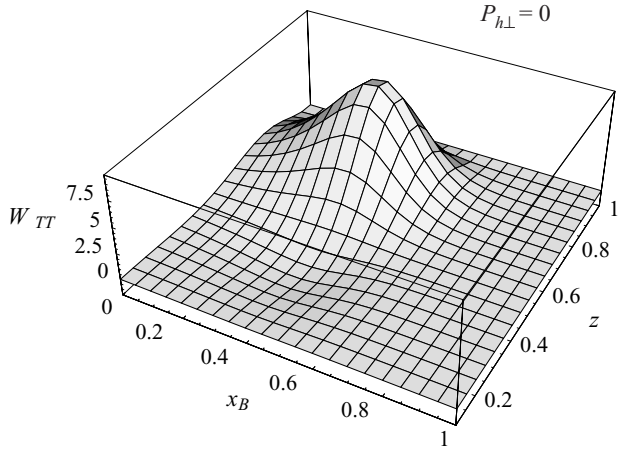

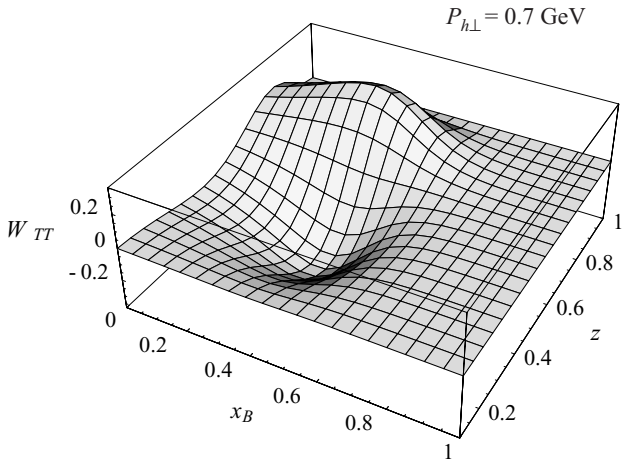

Fig. 14. Dependence of the structure function $W'^{[\mathrm{UL}]}_{TT}$ on x_B and z at two different values of $P_{h\perp}$.

Integrating over both z and x_B we obtain the dependence of the structure function $W'^{[\mathrm{UL}]}_{TT}$ on $P_{h\perp}$ alone (fig. 15).

5 – Unpolarized proton target and transversely polarized produced Λ. Substituting the results coming from eq. (33) and eq. (35) in the fourth term of eq. (22) and integrating over k_x and k_y we obtain

$$W'^{[\mathrm{UT}]}_{TT}(x_B, z, P_{h\perp}) = \sum_{i,j=s,a} c_{ij} \frac{n_i^2 N_j^2}{2M\,(2\pi)^6}\,(1-x_B)^3 \left(\frac{1-z}{z}\right)^3 \times \int \mathrm{d}p_x\,\mathrm{d}p_y \frac{p_x^2+p_y^2+(m+x_B M)^2}{\left[p_x^2+p_y^2+l_i^2(x)\right]^4} \times \frac{2\left(p_x-\frac{|P_{h\perp}|}{z}\right)\left(m+\frac{1}{z}M_h\right)}{\left[\left(p_x-\frac{|P_{h\perp}|}{z}\right)^2+p_y^2+L_j^2(z)\right]^4}. \quad (55)$$

Figure 16 shows the structure function $W'^{[\mathrm{UT}]}_{TT}$ (we plot $-W'^{[\mathrm{UT}]}_{TT}$ for display convenience) at $P_{h\perp} = 0.4$ GeV and $P_{h\perp} = 0.8$ GeV. Integrating over both z and x_B we obtain the dependence of the structure function $W'^{[\mathrm{UT}]}_{TT}$ on $P_{h\perp}$ alone (fig. 17).

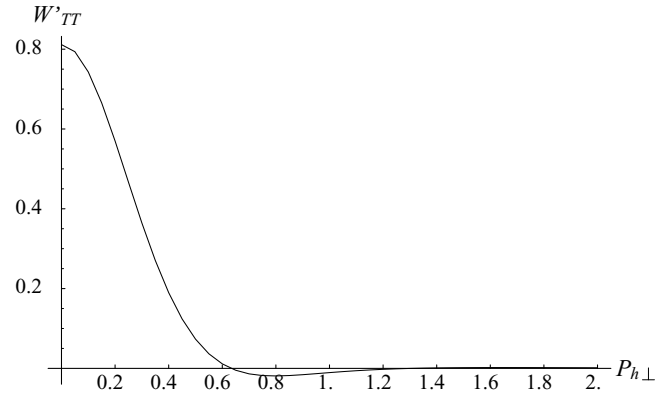

Fig. 15. Dependence of the structure function $W'^{[\mathrm{UL}]}_{TT}$ on the outgoing hadron transverse momentum, $P_{h\perp}$ (GeV).

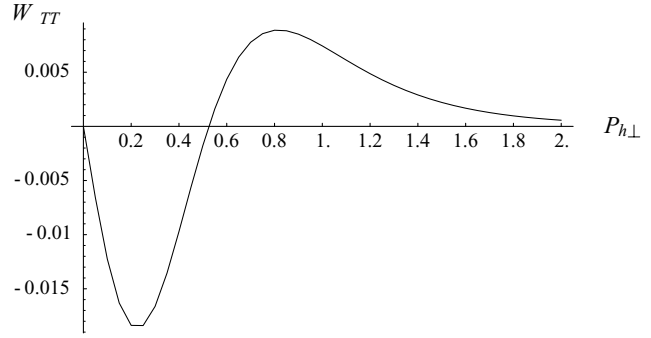

Fig. 17. Dependence of the structure function $W'^{[\mathrm{UT}]}_{TT}$ on the outgoing hadron transverse momentum, $P_{h\perp}$ (GeV).

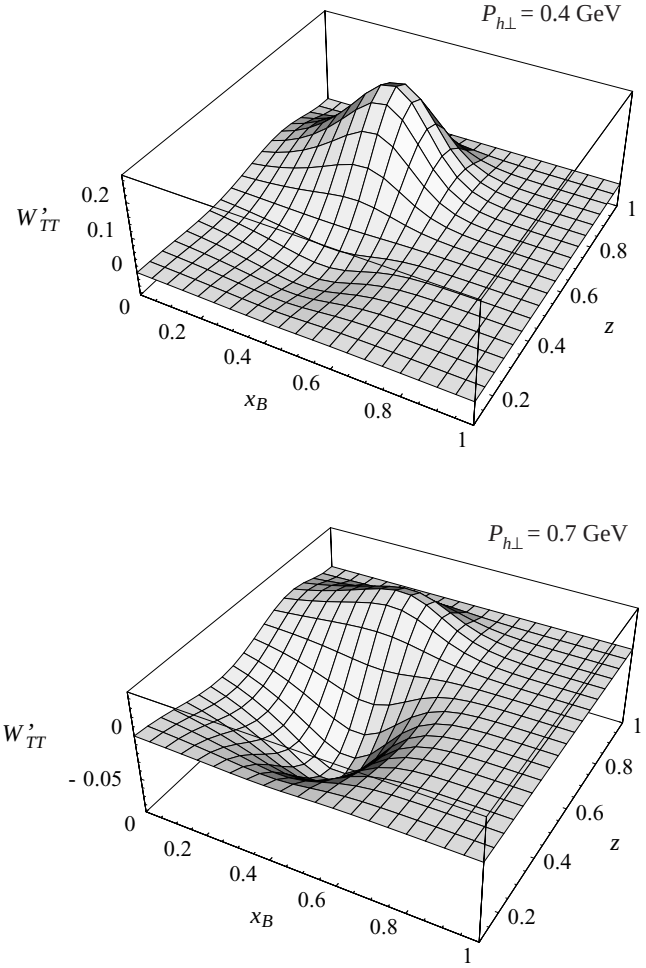

Fig. 16. Dependence of the structure function $-W'^{[\mathrm{UT}]}_{TT}$ on x_B and z at two different values of $P_{h\perp}$.

4 Conclusions

In this paper the structure functions appearing in the cross-section of polarized one-particle inclusive deep-inelastic scattering have been expressed in terms of distribution and fragmentation functions. Suitable kinematic conditions allow to extract selected structure functions and thus to access particular combinations of distribution and fragmentation functions.

We made use of a simple spectator model to calculate the relevant structure functions involved in the cross-section. Our analysis can be applied to any process involving a baryonic spin-$\frac{1}{2}$ target and an outgoing spin-$\frac{1}{2}$ baryon. We chose to focus our attention on the process $ep \to e'\Lambda X$. Using our results it is possible to estimate cross-sections for the cases when proton and Λ are both unpolarized or when one of the two is polarized.

An important feature of the analysis we presented is that we calculated the dependence of the cross-sections on the transverse momentum of the outgoing hadron, $P_{h\perp}$. The measurement of this variable gives access to two new contributions to the structure functions. These contributions have never been observed so far, because they vanish if the cross-section is integrated over $P_{h\perp}$. Furthermore, the dependence of the cross-section on $P_{h\perp}$ indirectly tests the distribution of partonic transverse momentum inside the hadron. This distribution is largely unknown at the moment.

The spectator model allows to study $P_{h\perp}$-dependent cross-sections because it produces a well-defined, analytical form of transverse momentum distributions. Since the model qualitatively agrees with totally inclusive measurements, we expect it to give good hints on the $P_{h\perp}$ dependence, as well. As shown in a brief comparison, the resulting $P_{h\perp}$-dependence is significantly different from the one predicted for instance by a Gaussian ansatz.

In summary, we are confident that the presented estimate can reproduce the broad features of the structure functions observable in semi-inclusive deep inelastic scattering.

This work is supported by the Foundation for Fundamental Research on Matter (FOM) and the Dutch Organization for Scientific Research (NWO) and was partly performed under contract ERB FMRX-CT96-0008 within the frame of the Training and Mobility of Researchers Program of the European Union.

References

1. European Muon Collaboration (M. Arneodo et al.), Nucl. Phys. B **321**, 541 (1989).
2. P.J. Mulders, R.D. Tangerman, Nucl. Phys. B **461**, 197 (1996).
3. R. Jakob, P.J. Mulders, J. Rodrigues, Nucl. Phys. A **626**, 937 (1997).
4. J.C. Collins, Nucl. Phys. B **396**, 161 (1993).
5. J. Levelt, P.J. Mulders, Phys. Rev. D **49**, 96 (1994).
6. S. Boffi, C. Giusti, F.D. Pacati, Phys. Rep. **226**, 1 (1993).
7. H. Arenhoevel, K.-M. Schmitt, Few-Body Systems **8**, 77 (1990).
8. J.P. Ralston, D.E. Soper, Nucl. Phys. B **152**, 109 (1979); J.C. Collins, D.E. Soper, Nucl. Phys. B **194**, 445 (1982).
9. D. Boer and P. J. Mulders, Nucl. Phys. B **569**, 505 (2000).
10. R. Jakob, P. Kroll, M. Schürmann and W. Schweiger, Z. Phys. A **347**, 109 (1993)